Microwave spectrum, dipole moment, structure, and internal rotation of the cyclopropanesulfur dioxide van der Waals complex

Anne M. Andrews, Kurt W. Hillig II, and Robert L. Kuczkowski

Citation: The Journal of Chemical Physics **96**, 1784 (1992); doi: 10.1063/1.462134
View online: http://dx.doi.org/10.1063/1.462134
View Table of Contents: http://scitation.aip.org/content/aip/journal/jcp/96/3?ver=pdfcov
Published by the AIP Publishing

Microwave spectrum, dipole moment, structure, and internal rotation of the cyclopropane-sulfur dioxide van der Waals complex

Anne M. Andrews, Kurt W. Hillig II, and Robert L. Kuczkowski
Department of Chemistry, University of Michigan, Ann Arbor, Michigan 48109-1055

(Received 29 July 1991; accepted 23 October 1991)

The rotational spectrum of the cyclopropane-sulfur dioxide complex was observed by Fourier transform microwave spectroscopy. The spectrum exhibited *a*- and *c*-dipole selection rules with the *c*-dipole transitions split into doublets of unequal intensity separated by about 150 kHz. The structure has C_s symmetry with the sulfur and carbon atoms all lying in the *ac* plane; the oxygen and hydrogen atoms straddle the plane. The sulfur dioxide plane is nearly parallel to a C–C bond edge. The distance from the center of mass of the SO_2 to the C–C bond center is 3.295 Å. The dipole moment of the complex is 1.681(1) D, with components $\mu_a = 0.815(1)$ D and $\mu_c = 1.470(1)$ D. The splittings in the spectrum arise from an internal rotation of the cyclopropane subunit about its local C_2 axis which lies nearly along the line connecting the centers of mass.

I. INTRODUCTION

Complexes of HF, HCl, and HCN with the hydrocarbon series ethylene,[1-3] acetylene,[4-6] and cyclopropane[7-9] have been studied recently. In each complex, the acid is hydrogen bonded to the π (ethylene and acetylene) or pseudo-π (cyclopropane) system.[10] It has been noted that for each HX series there is a decrease in hydrogen-bond length, an increase in pseudodiatomic stretching force constant, and an increase in induced dipole moment from ethylene to acetylene to cyclopropane.[11,12] As these properties are often correlated with the strength of the interaction, this has led to a discussion that the pseudo-π system of cyclopropane forms stronger hydrogen bonds than the classical π systems of ethylene and acetylene. Legon and Millen, studying the pseudodiatomic force constants of the HCl and HCN series, have assigned nucleophilicities to C_2H_4 (4.7), C_2H_2 (5.1), and C_3H_6 (6.4).[12]

While these trends are well documented for the hydrocarbon-acid complexes, which are hydrogen bonded, there is less data for this hydrocarbon series complexed to a non-hydrogen-bonding partner. Recently in our lab the complexes of ethylene and acetylene with sulfur dioxide have been observed.[13,14] In both cases, the complexes have a stacked structure with the C_2 axis of the SO_2 crossed at 90° to the C=C or C≡C bond. The sulfur of the SO_2 apparently interacts with the π system of the ethylene and acetylene. Like the acid complexes, it was observed that the interaction distance, as measured from the C–C bond center to the sulfur, is shorter for $C_2H_2 \cdot SO_2$ (3.359 Å) than $C_2H_4 \cdot SO_2$ (3.446 Å) and that the induced dipole moment is greater for $C_2H_2 \cdot SO_2$. The force constants for the stretching vibration between the hydrocarbon and the SO_2 are not easily compared due to the effect of internal rotation in $C_2H_4 \cdot SO_2$. This is discussed in Ref. 14.

Here we report on the cyclopropane·SO_2 ($C_3H_6 \cdot SO_2$) complex. The sulfur atom interacts with the pseudo-π system as expected, however, the structure is slightly different from the $C_2H_4 \cdot SO_2$ and $C_2H_2 \cdot SO_2$ complexes in that the C_2 axis of the SO_2 is nearly parallel to the C–C bond, rather than crossed at 90°. The interaction distance (S to C–C bond center) of 3.203 Å is shorter than in $C_2H_2 \cdot SO_2$. Moreover, the induced dipole moment and the pseudodiatomic force constant are both greater.

II. EXPERIMENT

A. Spectrometer

The spectrum was observed in a Fourier transform microwave spectrometer of the Balle–Flygare type which has been described previously.[15,16] The molecular beam was generated with a modified Bosch fuel injector. Linewidths were typically 20–30 kHz full width at half maximum (FWHM) and center frequencies were estimated to be accurate to ± 2–3 kHz. For deuterated isotopomers, transitions were broadened to 100 kHz or more from unresolved nuclear quadrupole hyperfine structure and line centers were accurate to ± 20–30 kHz. Stark effects were measured by applying up to 10 000 V with opposite polarities to two parallel steel mesh plates separated by about 30 cm.

B. Samples

The spectrum of $C_3H_6 \cdot SO_2$ was observed with a mixture of approximately 1% each of C_3H_6 (Aldrich) and SO_2 (Matheson) in Ar at a total pressure of 1.5 atm. $S^{18}O_2$ (98% ^{18}O) was purchased from Alfa Products and used without dilution to observe the $C_3H_6 \cdot S^{18}O_2$ spectrum. A 50:50 mixture of $S^{18}O_2$ and $S^{16}O_2$ was used to produce the $C_3H_6 \cdot S^{18}O^{16}O$ spectrum; the samples exchanged immediately upon mixing. The $C_3H_6 \cdot {}^{34}SO_2$ spectrum was observed in natural abundance (4% ^{34}S). C_3D_6 (98% D) and 1,1-$C_3H_4D_2$ (98%) were purchased from MSD isotopes.

C_3H_5D was synthesized in poor yield as follows. Cyclopropyl Grignard reagent was produced by reacting cyclopropyl bromide (Aldrich) with Mg (Baker) in dry diethyl ether in the usual manner. The flask containing the Grignard reagent was then placed in line with a trap cooled with a CCl_4 slush (− 25 °C) followed by a liquid-nitrogen trap (− 196 °C) which was isolated from the atmosphere by a mercury bubbler. Nitrogen gas was passed through the apparatus while D_2O (Cambridge Isotope Lab) was slowly

 0021-9606/92/031784-09$06.00

TABLE I. Observed transitions in MHz of $C_3H_6 \cdot SO_2$.

$J'_{K_pK_0}$	$J''_{K_pK_0}$	A_1/A_2[a]	$J'_{K_pK_0}$	$J''_{K_pK_0}$	A_1/A_2
3_{03}	2_{02}	7 311.753	5_{23}	4_{22}	12 207.788
3_{22}	2_{21}	7 315.089	5_{14}	4_{13}	12 383.484
3_{21}	2_{20}	7 318.850	6_{16}	5_{15}	14 387.127
3_{12}	2_{11}	7 432.386	6_{06}	5_{05}	14 597.283
4_{14}	3_{13}	9 595.002	6_{15}	5_{14}	14 856.965
4_{04}	3_{03}	9 744.449	7_{17}	6_{16}	16 780.978
4_{23}	3_{22}	9 752.487	7_{07}	6_{06}	17 015.605
4_{32}	3_{31}	9 754.511	7_{16}	6_{15}	17 382.667
4_{31}	3_{30}	9 754.584	2_{21}	2_{11}	14 754.456
4_{22}	3_{21}	9 761.865	2_{20}	2_{12}	14 990.582
4_{13}	3_{12}	9 908.517	3_{21}	3_{13}	15 112.216
5_{15}	4_{14}	11 991.722	4_{22}	4_{14}	15 279.080
5_{05}	4_{04}	12 173.271	5_{23}	5_{15}	15 495.147
5_{24}	4_{23}	12 189.058			
		A_2 (strong)			A_1 (weak)
1_{10}	0_{00}	7 435.084			7 435.245
2_{11}	1_{01}	9 951.926			9 952.070
3_{12}	2_{02}	12 508.184			12 508.346
4_{13}	3_{03}	15 104.949			15 105.104
6_{06}	5_{14}	9 026.565			9 026.412
7_{07}	6_{15}	11 185.201			11 185.039

[a] Symmetry designation of tunneling doublets. A_1/A_2 indicates that the transition was unsplit.

added dropwise to the cyclopropyl Grignard. Excess D_2O and ether were trapped in the CCl_4 trap and a small amount of C_3H_5D was collected in the liquid-nitrogen trap.

III. RESULTS AND ANALYSIS

A. Spectrum

The spectrum of $C_3H_6 \cdot SO_2$ exhibited *a*- and *c*-dipole selection rules. The *c*-type *R*-branch transitions were split into doublets of unequal intensity and the strong and weak *c*-type transitions were each fit independently with the *a*-type transitions to a Watson *S*-reduced Hamiltonian.[17] The observed transitions are listed in Table I and the derived constants are shown in Table II. The splitting of the *c*-type transitions arises from an internal rotation of the cyclopropane subunit exchanging three pairs of protons (see internal rotation section below) and the A_1 and A_2 symmetry labels of the states are taken by analogy to ethylene$\cdot SO_2$ which has a similar tunneling path.[13] For $C_3H_6 \cdot SO_2$, the A_1 label corresponds to the weaker transitions and the A_2 to the stronger. Additional effects of the internal rotation are seen in the difference in the sign of the D_K distortion constant between the A_1 and A_2 states. A similar effect was observed in the ethylene$\cdot SO_2$ complex and it is believed to arise from neglect of an internal rotation term in the Hamiltonian.

The spectra of $C_3H_6 \cdot {}^{34}SO_2$, $C_3H_6 \cdot S^{18}O_2$, and $C_3H_6 \cdot S^{18}O^{16}O$ were also all split into doublets, with the same relative intensity pattern as the normal isotopic species. For $C_3H_6 \cdot S^{18}O_2$ and $C_3H_6 \cdot S^{18}O^{16}O$, the magnitude of the splitting of the 2_{11}-1_{01} transitions decreased by 30% and 10%, respectively. For $C_3H_6 \cdot {}^{34}SO_2$, the splitting increased by 10%. In the $C_3D_6 \cdot SO_2$, the doublets were unresolved due to deuterium nuclear quadrupole broadening. For $C_3H_5D \cdot SO_2$ the transitions were unsplit. Two different spectra were observed for the 1,1-$C_3H_4D_2 \cdot SO_2$ isotopic species; one was split into doublets (labeled *apical*) and the other was unsplit (labeled *basal*). These labels will be dis-

TABLE II. Spectroscopic constants (Watson *S* reduction; I^r representation) of $C_3H_6 \cdot SO_2$.

	A_2[a]	A_1
A/MHz	6176.635(5)[b]	6176.828(5)
B/MHz	1258.500(1)	1258.500(1)
C/MHz	1180.101(1)	1180.101(1)
D_J/kHz	1.958(5)	1.959(6)
D_{JK}/kHz	15.5(1)	15.4(2)
D_K/kHz	−18.1(9)	20.5(11)
d_1/kHz	−0.078(4)	−0.077(5)
d_2/kHz	0.179(6)	0.178(7)
H_{KJ}/kHz	0.9(1)	0.8(2)
h_3/kHz	0.04(1)	0.04(1)
n[c]	33	33
$\Delta\nu_{rms}$[d]/kHz	6	7
μ_a/D	0.815(1)	
μ_c/D	1.470(1)	
μ_T/D	1.681(1)	

[a] Symmetry label of tunneling state (see text).
[b] Uncertainties represent 1σ in the least-squares fit.
[c] Number of transitions in the fit.
[d] $\Delta\nu = \nu_{obs} - \nu_{calc}$.

TABLE III. Observed transitions of cyclopropane-SO_2 isotopic species (in MHz).

$J'_{K_a K_c} - J''_{K_a K_c}$	$C_3H_6 \cdot {}^{34}SO_2$		$C_3H_6 \cdot S^{18}O^{16}O$		$C_3H_6 \cdot S^{18}O_2$		$C_2H_4D_2 \cdot SO_2$ *capical*[b]		$C_3D_6 \cdot SO_2$	$C_2H_5D \cdot SO_2$ *basal*[a]	$C_2H_4D_2 \cdot SO_2$ *basal*[a]
	A_2[c]	A_1	A_2	A_1	A_2	A_1	A_2	A_1	A_1/A_2[d]		
1_{10}-0_{00}	7403.587	7403.741								7311.752	
2_{11}-1_{01}	9894.945	9895.104	9676.028	9676.158	9407.874	9407.978	9589.050	9589.150	8851.200	9809.891	9577.077
3_{12}-2_{02}	12 424.588	12 424.744	12 205.618	12 205.749	11 912.787	11 912.891	11 985.335	11 985.441	11 168.850		12 093.137
4_{13}-3_{03}	14 993.558	14 993.719	14 778.921	14 779.036	14 464.672	14 464.763	14 419.172	14 419.282	13 517.715		14 646.758
5_{14}-4_{04}									15 899.180		
2_{20}-2_{12}											14 072.658
3_{21}-3_{13}									13 108.825		14 185.448
3_{03}-2_{02}		7242.123		7204.747							
3_{22}-2_{21}				7208.844					12 740.400	7263.862	
3_{21}-2_{20}				7213.358							
3_{12}-2_{11}		7359.271		7334.698		7242.826				7380.262	
4_{14}-3_{13}		9506.431		9441.707		9295.386		9000.566	8781.476	9536.547	9480.090
4_{04}-3_{03}		9651.854		9600.896		9464.759		9139.714	8898.074	9680.765	9618.737
4_{23}-3_{22}				9610.684		9476.560		8903.725	9146.734		9626.160
4_{22}-3_{21}				9621.962		9490.029		8910.253	9154.891		9634.778
4_{13}-3_{12}		9811.094		9778.040		9655.286		9291.601	9024.846	9839.058	9770.806
5_{15}-4_{14}		11 881.103		11 799.390		11 616.492		11 248.950	10 975.387	11 918.715	11 848.225
5_{05}-4_{04}		12 057.907		11 992.417		11 820.635		11 418.305	11 117.481	12 093.932	12 016.714
5_{24}-4_{23}								11 432.093	11 128.502		12 031.243
5_{23}-4_{22}								11 448.382	11 141.545		
5_{14}-4_{13}		12 261.818		12 220.021		12 066.153		11 615.640	11 279.513	12 296.731	12 211.498
6_{16}-5_{15}				14 155.851					13 168.348		14 215.132
6_{06}-5_{05}		14 459.410		14 378.225		14 169.756		13 692.702	13 333.516		14 410.259
6_{25}-5_{24}								13 716.568	13 352.544		14 435.352
6_{24}-5_{23}								13 745.006	13 375.327		
6_{15}-5_{14}									13 533.130		14 650.816
7_{17}-6_{16}									15 360.197		
7_{07}-6_{06}									15 545.550		

[a] D_1 or D_2 substitution at the C atom closest to the SO_2 (see Fig. 2). Only a singlet was observed.

[b] D_2 substitution at the C atom most distant from the SO_2 (see Fig. 2).

[c] Symmetry label of tunneling state (see text).

[d] Tunneling doublets not resolved.

TABLE IV. Spectroscopic constants for $C_3H_6 \cdot SO_2$ isotopic species.

	Symmetry[a]	A/MHz	B/MHz	C/MHz	n[b]	$\Delta\nu_{rms}$[c]
$C_3H_6 \cdot SO_2$	A_1	6176.635(5)[d]	1258.500(1)	1180.101(1)	33	6
	A_2	6176.828(5)	1258.500(1)	1180.101(1)	33	7
$C_3H_6 \cdot {}^{34}SO_2$	A_1	6157.911(7)	1245.746(2)	1169.572(2)	13	9
	A_2	6158.066(7)	1245.745(2)	1169.571(2)	13	10
$C_3H_6 \cdot S^{18}O_2$	A_1	5718.558(2)	1229.851(1)	1139.843(1)	13	11
	A_2	5718.664(4)	1229.850(1)	1139.845(1)	13	3
$C_3H_6 \cdot S^{18}O^{16}O$	A_1	5945.214(3)	1243.685(1)	1159.500(1)	17	3
	A_2	5945.345(3)	1243.684(1)	1159.501(1)	17	2
1,1-$C_3H_4D_2 \cdot SO_2$ (*apical*)[f]	A_1	6049.426(5)	1179.925(1)	1107.162(1)	16	6
	A_2	6049.523(5)	1179.926(1)	1107.162(1)	15	5
$C_3D_6 \cdot SO_2$	A_1/A_2[e]	5420.840(57)	1143.558(1)	1082.701(1)	30	6
$C_3H_5D \cdot SO_2$ (*basal*)[g]		6062.694(14)	1249.091(3)	1173.458(4)	10	18
1,1-$C_3H_4D_2 \cdot SO_2$ (*basal*)[f,g]		5857.749(6)	1239.833(1)	1167.135(1)	19	4

[a] Symmetry label of tunneling state (see text).
[b] Number of transitions in fit.
[c] $\Delta\nu = \nu_{obs} - \nu_{calc}$.
[d] Uncertainty is 1σ.
[e] Tunneling doublets not resolved for $C_3D_6 \cdot SO_2$.
[f] See footnote to Table III for explanation of *apical* and *basal* labels for 1,1-$C_3H_4D_2 \cdot SO_2$.
[g] No tunneling doublets observed for these isotopomers.

cussed in Sec. III C. For the spectrum of the *apical* species both tunneling doublets were very weak, making it difficult to assign strong and weak components. Therefore, the symmetry labels were assigned by higher/lower frequency to be consistent with the other isotopic species. The magnitude of the splitting decreased by 30%. The transitions for the isotopomers are listed in Table III and the rotational constants are given in Table IV; because the fitted distortion constants were similar to those for the normal isotopic form, only A, B, and C are reported for the isotopomers.

B. Dipole moments

The dipole moment of the complex was measured by tracking the Stark effect of seven M components from four transitions with increasing electric field. The electric field was calibrated using the $J = 1 \leftarrow 0$, $M = 0 \leftarrow 0$ transition of OCS at 12 162.980 MHz.[18] The observed Stark effects were least-squares fit to dipole components $\mu_a = 0.815(1)$ D and $\mu_c = 1.470(1)$ D resulting in $\mu_T = 1.681(1)$ D. When μ_b was included in the fit, the value for μ_b^2 was 0.030(50) D, indicating that μ_b was zero. The dipole moment components of *basal*-$C_3H_4D_2 \cdot SO_2$ were also determined as $\mu_a = 0.803(3)$ D and $\mu_c = 1.482(3)$ D from six M components from two transitions.

C. Structure

It was assumed in the structural analysis that the geometries of the cyclopropane and sulfur dioxide were not changed upon complexation from their free gas-phase structures.[19,20] The moments of inertia and planar second moments of the stronger set of transitions were used for the isotopic species which exhibited splittings. Because the difference in rotational constants is very small (< 200 kHz), this choice will not markedly affect the determination of the structure. The planar moments for $C_3H_6 \cdot SO_2$, $C_3H_6 \cdot {}^{34}SO_2$, cyclopropane, and sulfur dioxide are listed in Table V.

The a- and c-type selection rules and the absence of evidence for a μ_b dipole component suggest that the complex has an ac symmetry plane. Comparison of the planar moment P_{bb} of $C_3H_6 \cdot SO_2$ (54.2495 amu Å^2) with P_{bb} of $C_3H_6 \cdot {}^{34}SO_2$ (54.2460 amu Å^2) indicates that the S atom lies in this plane. P_{bb} for the complex is also equal to the sum of P_{aa} of free SO_2 and P_{cc} of free cyclopropane, placing the

TABLE V. Planar second moments [$P_{aa} = 0.5\ (I_c + I_b - I_a) = \Sigma m_i a_i^2$ and similarly for P_{bb}, P_{cc}] of cyclopropane-SO_2, cyclopropane and sulfur dioxide.

	$C_3H_6 \cdot SO_2$	$C_3H_6 \cdot {}^{34}SO_2$	Cyclopropane	SO_2
P_{aa}/amu Å^2	374.0012	377.8599	20.1254	48.7679
P_{bb}/amu Å^2	54.2495	54.2460	20.1254	8.3574
P_{cc}/amu Å^2	27.5716	27.8239	5.0262	0.0

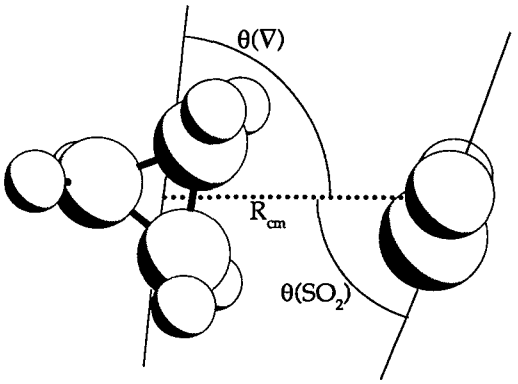

FIG. 1. Definition of structural parameters for cyclopropane·SO_2. $R_{c.m.}$ is the distance from between the centers of mass, $\theta(\nabla)$ is the angle between $R_{c.m.}$ and the line parallel to the bonded C–C bond running through the center of mass of cyclopropane, and $\theta(SO_2)$ is the angle between the C_2 axis of SO_2 and $R_{c.m.}$.

C_2 axis of SO_2 and the *ab* plane of cyclopropane in the *ac* plane of the complex. This orientation is shown in Fig. 1 with the S and C atoms in the *ac* symmetry plane and the O and H atoms straddling it. Once this is established, the geometry of the complex can be described by the three coordinates in Fig. 1: $R_{c.m.}$, the distance between the centers of mass of the SO_2 and the cyclopropane; $\theta(SO_2)$, the angle between the C_2 axis of SO_2 and $R_{c.m.}$; $\theta(\nabla)$, the angle subtended by $R_{c.m.}$ and a line through the center of mass of cyclopropane parallel to the C–C bond to which the SO_2 is bonded. These angles define the tilt of the cyclopropane or the SO_2 from perpendicular to $R_{c.m.}$, i.e., $\theta(\nabla) = \theta(SO_2) = 90°$ corresponds to no tilt.

With the symmetry of the molecule deduced, a brief comment about the spectra of the deuterated isotopes is appropriate before proceeding with a discussion of the structure. The relative orientation of the cyclopropane and the SO_2 permits three different isomers to exist for both $C_3H_5D\cdot SO_2$ and $C_3H_4D_2\cdot SO_2$. In each case the isotopic substitution could be on either of the CH_2 groups in the C–C bond which is closest to the SO_2 (labeled *basal* species), or on the CH_2 group opposite that bond (*apical*). In the case of $C_3H_5D\cdot SO_2$, due to difficulties with the synthesis, only one spectrum was observed before the sample was depleted. The rotational constants indicated that it was one of the *basal* isomers. For the $C_3H_4D_2\cdot SO_2$, two spectra were observed: one was consistent with the D_2 in the *apical* position and the other with D_2 in one of the *basal* positions. Although efforts were made to find the spectrum of the third species, it was not observed.

Little information could be gleaned from the moments of inertia of the normal isotopic species alone. Because the *b* coordinates of all the atoms are fixed by symmetry and the geometries of the monomers, only the P_{aa} and P_{cc} moments of inertia are useful for structure determination. The result is that $R_{c.m.}$ can be determined from I_b as approximately 3.73 Å but a series of correlated values for $\theta(SO_2)$ and $\theta(\nabla)$ are obtained from a single isotopic species.

In determining the structure by least-squares fitting of the moments of inertia of all the isotopic species, a choice must be made about assignment of the $C_3H_4D_2\cdot SO_2$ isotopic spectra. The assignment of one spectrum to the species substituted at the *apical* position and one substituted at the *basal* position was unambiguous based on the isotope shifts. However, the latter could be assigned to the CD_2 group either at the S or O atom side of the SO_2 (see Fig. 1). The same ambiguity occurs in the location of the *basal* deuterium in the $C_3H_5D\cdot SO_2$. Both assignments were tried and they resulted in the two fits shown in Table VI. It was evident that the CH_2–CD_2 or CH_2–CHD bond is tilted slightly to the SO_2 and that the D_2 (or D_1) substitution occurs at the carbon closer to the SO_2. The quality of the fits is similar because the coordinates of the deuterium are nearly identical in both structures.

Kraitchman's equations were used to calculate the positions of the substituted atoms.[21] They are compared with the values from the least-squared fit in Table VI. The coordinates determined for the $C_3H_5D\cdot SO_2$ species and the *basal*-$C_3H_4D_2\cdot SO_2$ species are the same and indicate the *basal* substitution with the CD_2 group nearer the SO_2. The coordinates determined for the *apical*-$C_3H_4D_2\cdot SO_2$ species place the hydrogen atom near to the *a* axis and much further from the SO_2. The substitution coordinates do not, however, distinguish between the two structures. The S and O coordinates from Kraitchman's equations are included in Table VI for completeness.

A similar ambiguity about the sign of an angle was encountered in the $C_2H_4\cdot SO_2$ complex, where the tilt angle of the ethylene was difficult to determine.[13] This was resolved by examining the change in the dipole moment projections

TABLE VI. Structural parameters and atomic coordinates obtained from least-squares fitting of moments of inertia and Kraitchman equations.

		Fit 1[a]	Fit 2[a]	Kraitchman
R_{cm}/Å[b]		3.729(1)	3.729(1)	
$\theta(SO_2)$/deg		73.2(1.7)	73.3(1.7)	
$\theta(\nabla)$/deg		83.3(2.4)	96.8(2.4)	
ΔI_{rms}/amu Å^2		0.52	0.52	
S	*a*	1.37 Å	1.38 Å	1.40 Å
	b	0.0	0.0	0.0
	c	0.36	0.36	0.36
O	*a*	1.58	1.58	1.52
	b	1.24	1.24	1.24
	c	0.38	0.38	0.32
H[c] (*basal*)	*a*	1.38	1.39	1.26[e]
	b	0.91	0.91	0.89
	c	1.17	1.15	1.21
H[d] (*apical*)	*a*	3.69	3.69	3.67[e]
	b	0.91	0.91	0.89
	c	0.19	0.15	0.26

[a] Least-squares fit of 24 moments of inertia (A_2 symmetry state) from the eight isotopic species in Table IV. Fit 1 is preferred by the authors (see text).

[b] See Fig. 1 for definition of coordinates.

[c] H (*basal*) is the hydrogen at the carbon position in the CH_2–CH_2 bond which is closest to the SO_2 (see Fig. 2).

[d] H (*apical*) is the hydrogen at the carbon most distant from the SO_2 (see Fig. 2).

[e] Calculated from the 1,1-$C_3H_4D_2\cdot SO_2$ species.

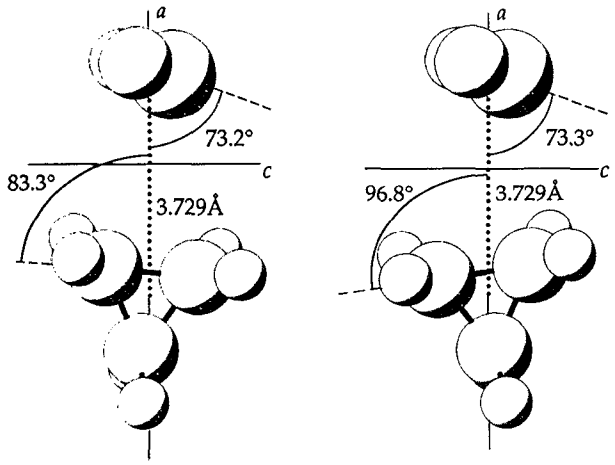

FIG. 2. Two structures of cyclopropane·SO_2 determined from least-squares fitting of the moments of inertia. The structure on the left with $\theta(\nabla) = 83.3°$ is preferred.

upon isotopic substitution. A similar analysis was employed here. When a molecule is isotopically substituted, its principal inertial axes translate and rotate. The result of the rotation is a small change in the projections of the dipole moment on the principal axes. It is assumed that the change in the total dipole moment upon isotopic substitution is negligible.

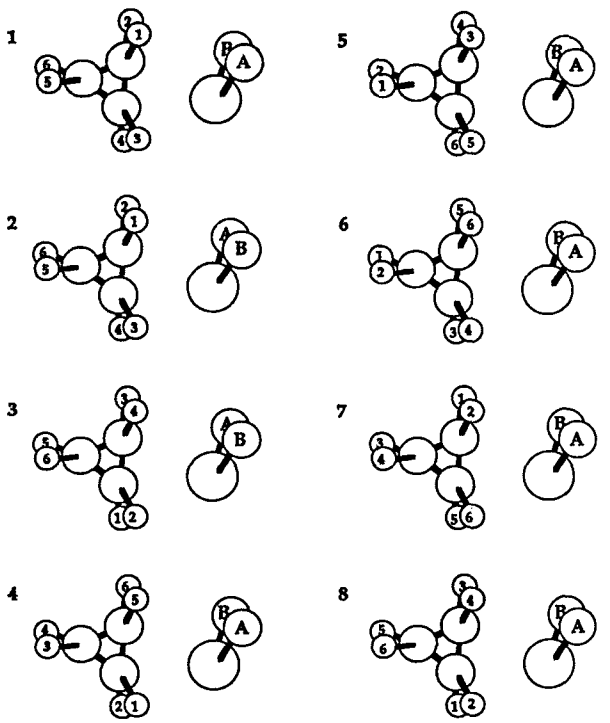

FIG. 3. Feasible permutation of nuclei which were considered to account for tunneling splittings in the spectrum of $C_3H_6 \cdot SO_2$. Permutations and likely pathways are $1 \rightarrow 2$ (ab), rotation of SO_2 about its local C_2 axis; $1 \rightarrow 3$ $(ab)(14)(23)(56)$, inversion of SO_2; $1 \rightarrow 4$ $(135)(246)$ and $1 \rightarrow 5$ $(153)(264)$, rotation of cyclopropane about its C_3 axis; $1 \rightarrow 6$ $(34)(16)(25)$, $1 \rightarrow 7$ $(12)(36)(45)$, and $1 \rightarrow 8$ $(14)(23)(56)$, rotations of cyclopropane about each of its C_2 axes.

TABLE VII. Predicted and observed dipole moments for *basal*-1,1-$C_3H_4D_2 \cdot SO_2$ for the two structures with $\theta(\nabla) = 83.3°$ and $\theta(\nabla) = 96.8°$.

	$\theta(\nabla) = 83.3°$	$\theta(\nabla) = 96.8°$	Obs.
μ_a/D	0.802	0.829	0.803(3)
μ_c/D	1.478	1.463	1.482(3)

This should be a reasonable assumption for $C_3H_4D_2 \cdot SO_2$. The dipole moment of 1,1-$C_3H_4D_2$ has been measured as 0.011(5) D,[22] and the total dipole moments of the $C_3H_4D_2 \cdot SO_2$ and $C_3H_6 \cdot SO_2$ differ by only 0.006(4) D. It is also assumed that the effect of vibrational averaging on the momomer and induced dipole moments is not dependent on the direction of $\theta(\nabla)$. A quantitative estimate of these effects is difficult. However, the success of the method in the $C_2H_4 \cdot SO_2$ problem, where several cross checks of the structure were available, suggests that averaging effects on the dipole moments can be neglected. The two options for the assignment of the *basal* CD_2 spectrum rotate the axes in opposite directions. For both rotations the *a*- and *c*-dipole components were predicted and they are shown in Table VII. The direction of the dipole moment of the complex is selected such that it is dominated by the permanent dipole moment of SO_2.[23] The observed dipole components for *basal*-$C_3H_4D_2 \cdot SO_2$ indicate $\theta(\nabla) = 83.3°$. The uncertainties for $R_{c.m.}$ and the tilt angles in Table VI are the statistical uncertainties arising from the fitting process. The structural parameters are the so-called r_0 values.[24] It is difficult to estimate how closely they approximate the equilibrium values due to the large amplitude vibrational motions in such complexes; it is probably reasonable to expect these values to be within $\pm$ 0.03 Å for $R_{c.m.}$ and $\pm$ 5° for the tilt angles.

D. Internal rotation

The splitting in the *c*-type transitions signifies that a tunneling motion occurs between two or more equivalent configurations in the complex. In an attempt to determine the tunneling path, the feasible permutations of identical nuclei shown in Fig. 3 were considered. Possible tunneling paths for the permutations are the following: $1 \rightarrow 2$, rotation of SO_2 about its C_2 axis; $1 \rightarrow 3$, inversion of SO_2 through a C_{2v} intermediate structure; $1 \rightarrow 4$ and $1 \rightarrow 5$, rotation of cyclopropane about its C_3 axis; $1 \rightarrow 6$ and $1 \rightarrow 7$, rotation of cyclopropane about either of its C_2 axes including the bond CH_2 groups (the symmetry arguments are the same for both); $1 \rightarrow 8$, rotation of cyclopropane about its C_2 axis including the apical CH_2 group.

The $1 \rightarrow 2$ and $1 \rightarrow 3$ motions can be eliminated as the source of the tunneling doublets based on the spectrum of the normal isotopic species. If the tunneling path were $1 \rightarrow 2$, two identical oxygen atoms ($I = 0$) would be exchanged and half the levels would have zero nuclear spin weight. For the $1 \rightarrow 3$ motion, the direction of the *c*-dipole moment reverses, resulting in *c*-dipole selection rules between the A_1 and A_2 symmetry states. Since the two sets of *c*-type transitions may be fit separately, the observed selection rules are inconsistent with this tunneling path.

The remaining tunneling paths involve the cyclopropane subunit, therefore, the deuterated isotopomers were instrumental in exploring them. From structural considerations alone, three isomers would be expected for the 1,1-$C_3H_4D_2 \cdot SO_2$: one with the CD_2 group in the *basal* position at the S of the SO_2, a second in the *basal* position at the O of the SO_2, and the third in the *apical* position. Referring to framework 1 in Fig. 3, these correspond to substitution in positions 3 and 4, positions 1 and 2, and positions 5 and 6, respectively. The tunneling paths under consideration, however, would result in different splitting patterns for the different isomers. For the $1 \rightarrow 4$ and $1 \rightarrow 5$ motions, rotation of cyclopropane about its C_3 axis, none of the $C_3H_4D_2 \cdot SO_2$ spectra should be split. This path would exchange the CD_2 group among three structurally inequivalent frameworks which have different moments of inertia. With the exception of $H^{35}Cl \cdot H^{37}Cl$, tunneling doublets are generally not observed under those conditions.[25] The $1 \rightarrow 6$ and $1 \rightarrow 7$ motions would produce a split spectrum for the *basal* CD_2 group on the C_2 axis about which the cyclopropane rotates as this would exchange identical nuclei. However, unsplit spectra would be expected for the the CD_2 group at the other *basal* and the *apical* positions. For the $1 \rightarrow 8$ path, the CD_2 group in the *apical* position results in the exchange of identical atoms and tunneling doublets, while both the *basal* CD_2 groups are distinct and would be unsplit. The observation of splittings in the spectrum of the CD_2 group in the *apical* position and an unsplit spectrum for the CD_2 group in the *basal* position then indicates that the $1 \rightarrow 8$ motion is the correct tunneling path. This would produce nuclear spin statistical weights of approximately 1:1.3 in the normal isotopic form and, although the relative intensities of the two states could not be measured, they are estimated to be between 1:1 and 1:2.

It should be noted that the $1 \rightarrow 8$ path is described as rotation of cyclopropane about its C_2 axis. This facilitates the discussion of the symmetry but does not necessarily imply that the SO_2 is a fixed framework on which the cyclopropane rotates. Although this division is common and a good description when the masses of the two parts are very different, such a separation is not obvious for $C_3H_6 \cdot SO_2$. Perhaps a geared rotation of the two subunits against one another would be a more appropriate description. There is some suggestion of this since the magnitude of the tunneling splitting is affected not only by isotopic substitution on the cyclopropane, but also on the sulfur dioxide. It is not trivial to estimate the barrier from the observed splittings and this was not attempted.

Finally, it is interesting that out of three possible structural isomers for 1,1-$C_3H_4D_2 \cdot SO_2$, only two were observed. While it is not uncommon under supersonically cooled beam conditions for only the isotopomer with the lowest zero-point energy to be populated,[26] the observation of two out of three isomers is puzzling. The tunneling path seems to shed some light on this. Based on statistical arguments, it is equally likely that the SO_2 will bond to any of the three C–C bonds in the 1,1-$C_3H_4D_2$ species when the complexes are formed in the nozzle. If the two bond positions have different zero-point energies, a path exists for cooling to the lower energy *basal* position through the tunneling coordinate, i.e., the internal rotation pathway is a means for equilibrating between the two CD_2 bond isomers. However, there is no ready pathway for cooling between the *basal* and *apical* positions if the barrier to exchange for this motion is very high, and both of these forms remain populated at the level determined by the beam kinetics.

IV. DISCUSSION

The structure of $C_3H_6 \cdot SO_2$ is similar to the structures of $C_2H_4 \cdot SO_2$ and $C_2H_2 \cdot SO_2$ in that the S atom is closest to the pseudo-π system of the cyclopropane. The symmetry, however, is different with the dihedral angle (α) between the C_2 axis of the SO_2 and the C–C bond equal to 0° for $C_3H_6 \cdot SO_2$ compared to 90° for $C_2H_4 \cdot SO_2$ and $C_2H_2 \cdot SO_2$. To explore whether this could be attributed to electrostatic considerations alone, the distributed multipole (DMA) model of Buckingham and Fowler was employed.[27] Distributed multipoles for SO_2 were taken directly from Buckingham and Fowler, while those for cyclopropane were calculated using the CADPAC program with a DZP (double zeta plus polarization) basis set.[28] The coordinates and multipoles are listed in Table VIII. The DMA gives a minimum of energy at the $\alpha = 0°$ geometry with $\theta(SO_2) = 90°$ and $\theta(\nabla) = 75°$, which are considerably different from the experimental angles. The well seems to be very shallow, however, and the experimental geometry $\theta(SO_2) = 74°$, $\theta(\nabla) = 84°$ is only 13 cm^{-1} higher in energy. The lowest-energy structure for $\alpha = 90°$ is 75 cm^{-1} higher in energy.

TABLE VIII. Cyclopropane distributed multipole moments in atomic units.

Site	x	y	z	q	μ_x[a]	μ_y	μ_z	θ_{xx}	θ_{yy}	θ_{zz}	θ_{yz}
C1	0.0	0.827	1.432	0.0845	0.0	−0.0908	−0.1711	−0.1331	0.4772	−0.3441	0.7112
C2	0.0	0.827	−1.432	0.0845	0.0	−0.0908	0.1711	−0.1331	0.4772	−0.3441	−0.7112
C3	0.0	−1.654	0.0	0.0845	0.0	0.1975	0.0	−0.7547	0.8879	−0.1331	0.0
H1	1.724	1.371	2.375	−0.0423	0.1487	0.0525	0.0909	0.0226	−0.0130	−0.0096	0.0
H2	1.724	1.371	−2.375	−0.0423	0.1487	0.0525	−0.0909	0.0226	−0.0130	−0.0096	0.0
H3	−1.724	−2.742	0.0	−0.0423	−0.1487	−0.1050	0.0	0.0226	−0.0109	−0.0116	0.0
H4	−1.724	1.371	2.375	−0.0423	−0.1487	0.0525	0.0909	0.0226	−0.0130	−0.0096	0.0
H5	−1.724	1.371	−2.375	−0.0423	−0.1487	0.0525	−0.0909	0.0226	−0.0130	−0.0096	0.0
H6	1.724	−2.742	0.0	−0.0423	0.1487	−0.1050	0.0	0.0226	−0.0109	−0.0116	0.0

[a] Dipole moment directions are from regions of negative to positive charge.

TABLE IX. Comparison of the complexes of cyclopropane, acetylene, and ethylene.

		Cyclopropane	Acetylene	Ethylene
SO_2	R/Å[a]	3.203	3.359	3.446
	k/mdyne Å^{-1}[b]	0.059	0.047	0.057
	ϵ/cm^{-1}[c]	652	390	490
	μ_a(ind)/D[d]	0.349	0.326	0.289
	μ_c(ind)/D[d]	0.095	0.063	0.072
	μ_I(ind)/D[d]	0.361	0.332	0.298
	Reference		14	13
HCl	R/Å	3.567	3.699	3.724
	k/mdyne Å^{-1}	0.087	0.067	0.061
	ϵ/cm^{-1}	959	614	575
	Reference	8	5	2
HCN	R/Å	3.475	3.656	3.711
	k/mdyne Å^{-1}	0.062	0.053	0.046
	ϵ/cm^{-1}	862	642	575
	Reference	9	6	3
HF	R/Å	3.021	3.121	3.143
	μ_{ind}/D	0.78	0.65	0.67
	Reference	7	4	1

[a] R is the distance from hydrocarbon C–C bond to nearest heavy atom.
[b] k is the pseudodiatomic stretching force constant.
[c] ϵ is the pseudodiatomic well depth.
[d] Induced dipole moment/D (see text).

The appropriate hydrocarbon·X distances, stretching force constants, well depths, and induced dipole moments for the cyclopropane, ethylene, and acetylene complexes with SO_2, HCl, HCN, and HF are shown in Table IX. The pseudodiatomic stretching force constant for $C_3H_6 \cdot SO_2$ was calculated using Millen's model[29] as 0.059 mdyne/Å and from this the binding energy was estimated as 650 cm^{-1}. The induced dipole moments for the HF complexes were taken from Nelson, Fraser, and Klemperer[11] as $\mu_{ind} = \mu - \langle \cos\theta \rangle \mu_{HF}$, where $\langle \cos\theta \rangle$ is approximated by $\langle \cos^2\theta \rangle^{1/2}$ which is determined from hyperfine interaction constants. For the SO_2 complexes an estimate of the averaging effects from bending motions on the dipole moments is not so straightforward as there are no hyperfine interactions giving information on the SO_2 bending vibration. These effects were neglected and the induced moments were taken as the difference between the observed dipole components and the projections of the SO_2 permanent dipole moment on the principal axes of the complex.

The SO_2 complexes exhibit the same decrease in sulfur to the C–C bond center distance previously noted for the hydrogen-bonded complexes. There is an increase in induced dipole moment in the series ethylene, acetylene, and cyclopropane, while in the HF complexes, the induced dipole moment is about the same for $C_2H_2 \cdot HF$ and $C_2H_4 \cdot HF$ and larger for $C_3H_6 \cdot HF$. The force constants and binding energies are also greater for $C_3H_6 \cdot SO_2$ than $C_2H_2 \cdot SO_2$. The values for $C_2H_4 \cdot SO_2$ are anomalously high, most probably because of perturbations in the spectrum due to a tunneling motion which contaminates the distortion constants. The difficulty with the $C_2H_4 \cdot SO_2$ distortion constants aside, it is reasonable to conclude from the other data that $C_3H_6 \cdot SO_2$ is the most strongly bound of the three, consistent with the finding of Legon and Millen that C_3H_6 is the best nucleophile.[12b]

Legon and Millen's model for determining nucleophilicities and electrophilicities has been successful in interpreting hydrogen-bonded complexes, but it has not yet been applied to other weak complexes. Because many SO_2 complexes have been characterized in recent years, the $C_xH_y \cdot SO_2$ complexes seemed an ideal situation to test it. The formula for relating nucleophilicities and electrophilicities to the pseudodiatomic stretching force constant is[12a]

$$k_\sigma = cNE$$

where k_σ is the force constant, c is a proportionality constant (equal to about 0.25), N is the nucleophilicity of the nucleophile, and E is the electrophilicity of the electrophile. Using $N = 6.4$ for cyclopropane as determined by Legon and Millen, E for SO_2 was calculated as 3.7. This was then used to predict k_σ for a number of SO_2 complexes with molecules for which the nucleophilicities have been calculated. These are shown in Table X along with the experimentally deter-

TABLE X. Pseudodiatomic stretching force constants for SO_2 containing complexes.

	$k_\sigma/10^{-2}$ mdyne Å^{-1}		
	Predicted[a]	Observed[b]	Reference
$C_3H_6 \cdot SO_2$[c]	5.9	5.9	
$C_2H_2 \cdot SO_2$	4.7	4.7	14
$H_2O \cdot SO_2$	9.3	8.4	32
$H_2S \cdot SO_2$	4.4	5.3	33
$HCN \cdot SO_2$	6.7	2.7	34
$(CH_3)_2O \cdot SO_2$	10.4	6.8	35

[a] Predicted using nucleophilicity from Ref. 12(b) and electrophilicity of $SO_2 = 3.7$ (see text).
[b] Obtained from D_J and pseudodiatomic approximation (Ref. 29).
[c] $C_3H_6 \cdot SO_2$ was used to determine the electrophilicity of SO_2; therefore, the match is required to be exact.

mined k_σ. There is excellent agreement for $C_2H_2 \cdot SO_2$ and quite good agreement for $SO_2 \cdot H_2O$ (Ref. 30) and $H_2S \cdot SO_2$ (Ref. 31). The agreement for $HCN \cdot SO_2$ (Ref. 32) and $(CH_3)_2O \cdot SO_2$ (Ref. 33) is rather poor. These complexes, however, are unusual in that the two subunits are somewhat closer than the sum of their van der Waals radii. In the case of $(CH_3)_2O \cdot SO_2$ the interaction may involve some charge-transfer interaction. This raises questions about the validity of the psuedodiatomic approximation, but also suggests that the nucleophilicity model is perhaps only applicable to complexes which are bound by primarily electrostatic forces. A larger data set is needed to test whether these complexes represent an anomaly or whether the model does not readily transfer to non-hydrogen-bonded weak complexes.

ACKNOWLEDGMENTS

This work was supported by a grant from the National Science Foundation. We are grateful for time granted at the San Diego Supercomputing Center. A.M.A. acknowledges the support of a Regents-Baer Fellowship at the University of Michigan.

[1] J. A. Shea and W. H. Flygare, J. Chem. Phys. **76**, 4857 (1982).
[2] S. G. Kukolich, P. D. Aldrich, W. G. Read, and E. J. Campbell, Chem. Phys. Lett. **90**, 329 (1982).
[3] S. G. Kukolich, W. G. Read, and P. D. Aldrich, J. Chem. Phys. **78**, 3552 (1983).
[4] W. G. Read and W. H. Flygare, J. Chem. Phys. **76**, 2238 (1982).
[5] A. C. Legon, P. D. Aldrich, and W. H. Flygare, J. Chem. Phys. **75**, 625 (1981).
[6] P. D. Aldrich, S. G. Kukolich, and E. J. Campbell, J. Chem. Phys. **78**, 3521 (1983).
[7] L. W. Buxton, P. D. Aldrich, J. A. Shea, A. C. Legon, and W. H. Flygare, J. Chem. Phys. **75**, 2681 (1981).
[8] A. C. Legon, P. D. Aldrich, and W. H. Flygare, J. Amer. Chem. Soc. **104**, 1486 (1982); P. D. Aldrich, S. G. Kukolich, E. J. Campbell, and W. G. Read, *ibid.* **105**, 5569 (1983).
[9] S. G. Kukolich, J. Chem. Phys. **78**, 4832 (1983).
[10] C. A. Coulson and W. E. Moffit, J. Chem. Phys. **15**, 151 (1947); C. A. Coulson and W. E. Moffit, Philos. Mag. **40**, 1 (1949).
[11] D. D. Nelson, Jr, G. T. Fraser, and W. Klemperer, J. Chem. Phys. **82**, 4483 (1985).
[12] (a) A. C. Legon and D. J. Millen, J. Amer. Chem. Soc. **109**, 356 (1987); (b) A. C. Legon and D. J. Millen, J. Chem. Soc. Chem. Comm. 986 (1987).
[13] A. M. Andrews, A. Taleb-Bendiab, M. S. LaBarge, K. W. Hillig II, and R. L. Kuczkowski, J. Chem. Phys. **93**, 7030 (1990).
[14] A. M. Andrews, K. W. Hillig, R. L. Kuczkowski, A. C. Legon, and N. W. Howard, J. Chem. Phys. **94**, 6946 (1991).
[15] T. J. Balle and W. H. Flygare, Rev. Sci. Instrum. **52**, 33 (1981).
[16] K. W. Hillig II, J. Matos, A. Scioli, and R. L. Kuczkowski, Chem. Phys. Lett. **133**, 359 (1987).
[17] J. K. G. Watson, J. Chem. Phys. **46**, 1935 (1967).
[18] K. Tanaka, H. Ito, K. Harada, and T. Tanaka, J. Phys. Chem. **80**, 5893 (1984).
[19] Y. Endo, M. C. Chang, and E. Hirota, J. Mol. Spec. **126**, 63 (1987).
[20] M. D. Harmony, V. W. Laurie, R. L. Kuczkowski, R. H. Schwendeman, D. A. Ramsey, F. J. Lovas, W. J. Lafferty, and A. G. Maki, J. Chem. Phys. Ref. Data **8**, 619 (1979).
[21] J. Kraitchman, Am J. Phys. **21**, 17 (1953); A. Chutjian, J. Mol. Spectrosc. **14**, 361 (1964).
[22] O. Böttcher, N. Heineking, and D. H. Sutter, J. Mol. Spec. **139**, 236 (1990).
[23] F. J. Lovas, J. Chem. Phys. Ref. Data, **14**, 395 (1985).
[24] R. H. Schwendeman, *Critical Evaluation of Chemical and Physical Structural Information*, edited by D. R. Lide and M. A. Paul (National Academy of Sciences, Washington, D. C., 1974), pp. 74–115.
[25] N. Ohashi and A. S. Pine, J. Chem. Phys. **81**, 73 (1984).
[26] T. R. Dyke, B. J. Howard, and W. Klemperer, J. Chem. Phys. **56**, 2442 (1972); H. S. Gutowsky, C. Chuang, J. D. Keen, T. D. Klots, and T. Emilsson, J. Chem. Phys. **83**, 2070 (1985).
[27] A. D. Buckingham and P. W. Fowler, Can. J. Chem. **63**, 2018 (1985).
[28] R. D. Amos and J. E. Rice, Cambridge Analytical Derivatives Package, Issue 4.0, Cambridge, 1987.
[29] D. J. Millen, Can. J. Chem. **63**, 1477 (1985).
[30] K. Matsumura, F. J. Lovas, and R. D. Suenram, J. Chem. Phys. **91**, 5887 (1989).
[31] R. E. Bumgarner, D. J. Pauley, and S. G. Kukolich, J. Chem. Phys. **87**, 3749 (1987); D. J. Pauley, and S. G. Kukolich, *ibid.* **93**, 1487 (1990).
[32] E. J. Goodwin and A. C. Legon, J. Chem. Phys. **85**, 6828 (1986).
[33] J. J. Oh, K. W. Hillig II, and R. L. Kuczkowski, Inorg. Chem. (to be published).